

# Diffractive hadron leptonproduction and SPD

S. V. GOLOSKOKOV

*Bogoliubov Laboratory of Theoretical Physics, Joint Institute for Nuclear Research*

Received 20 October 2002;  
final version 31 December 2003

We discuss diffractive hadron leptonproduction in terms of skewed gluon distributions and within two-gluon exchange model. Connection of the two-gluon approach with skewed gluon distributions is found. The double spin asymmetries for longitudinally polarized leptons and transversely polarized protons in diffractive vector meson and  $Q\bar{Q}$  production at high energies within the two-gluon model is analysed. The asymmetry predicted for meson production is found to be quite small. The  $A_{LT}$  asymmetry for  $Q\bar{Q}$  production is large and can be used to obtain information on the polarized skewed gluon distributions in the proton.

*PACS:* 12.38.Bx, 13.60.Hb

*Key words:* Diffraction, spin, asymmetry, hadron production

## 1 Introduction

In this lecture, we study diffractive hadron leptonproduction at high energies and small  $x$ . The scattering amplitude in this region is predominated by the two-gluon exchange which can be associated with the Pomeron. In diffractive reactions like vector meson and  $Q\bar{Q}$  production the momentum  $x_P$  carried by the two-gluon system is nonzero and the gluon momenta cannot be equal. Such processes can be expressed in terms of generalized or skewed parton distribution (SPD) in the nucleon  $\mathcal{F}_\zeta(x)$  where  $x$  is a fraction of the proton momentum carried by the outgoing gluon and  $\zeta$  is the difference between the gluon momenta (skewedness) [1]. For the processes which include light quarks, the  $q\bar{q}$  exchange in the  $t$ -channel should be important for  $x \geq 0.1$  in addition to the gluon contribution. For diffractive  $J/\Psi$  and charm quark production the predominated contribution is determined by the two-gluon exchange (gluon SPD). We shall mainly discuss here such reactions which should play a key role in future study of the gluon distribution  $\mathcal{F}_\zeta(x)$  at small  $x$ .

Intensive experimental study of diffractive processes was performed in DESY (see e.g. [2, 3, 4, 5]). The polarized observables in vector meson production were analysed in [6, 7]. Theoretical investigation of the diffractive vector meson production was conducted on the basis of the two-gluon exchange model where the typical scale  $\bar{Q}^2 = (Q^2 + M_V^2)/4$  was found for vector mesons production [8, 9]. The cross sections of light and heavy meson production plotted versus this variable look similar [10]. The amplitudes for longitudinally and transversely polarized photon were analyzed in [11, 12, 13]. The longitudinally polarized photon gives a predominant contribution to the cross section for  $Q^2 \rightarrow \infty$ . The cross section with transverse photon polarization is suppressed as a power of  $Q$ . Note that in the two-gluon model the imaginary part of the amplitude is usually calculated. The real part can be re-

produced [9] using the local dispersion relations. A more general SPD approach was applied to study the vector meson production by many authors (see e.g [14, 15]). Within the SPS approach, one can study simultaneously the imaginary and real parts of diffractive amplitudes. The double spin asymmetry for longitudinal photon and proton polarization in  $J/\Psi$  production was investigated in [16]. Theoretical analysis of the diffractive  $Q\bar{Q}$  production was carried out in [17, 18, 19, 20]. It was shown that the cross sections of diffractive quark- antiquark production were expressed in terms of the same gluon distributions as in the case of vector meson production.

This lecture is organized as follows. In the second section, we discuss the main features of the diffractive hadron leptonproduction processes and their connection with SPD. The two-gluon model approach and the spin structure of the two-gluon coupling with the proton are considered in section 3. The diffractive  $J/\Psi$  and charm quark pair production is analysed in sections 4, 5. The connection of the two-gluon approach with skewed gluon distributions is found here too. In sections 6 and 7 we consider double spin asymmetries for polarized leptons and protons in diffractive vector meson and  $Q\bar{Q}$  production at high energies. The predictions for the HERMES and COMPASS energies are made here.

## 2 Diffractive hadron production and SPD

Let us study the diffractive hadron production in lepton-proton reactions

$$l + p \rightarrow l + p + H \quad (1)$$

at high energies in a lepton-proton system. The hadron state  $H$  in this reaction can contain a vector meson or a  $Q\bar{Q}$  system which are observed as two final jets. The reaction (1) can be described in terms of the kinematic variables which are defined as follows:

$$q^2 = (l - l')^2 = -Q^2, \quad t = r_P^2 = (p - p')^2, \\ y = \frac{p \cdot q}{l \cdot p}, \quad x = \frac{Q^2}{2p \cdot q}, \quad x_P = \frac{q \cdot (p - p')}{q \cdot p}, \quad \beta = \frac{x}{x_P}, \quad (2)$$

where  $l, l'$  and  $p, p'$  are the initial and final lepton and proton momenta, respectively,  $Q^2$  is the photon virtuality, and  $r_P$  is the momentum carried by the two-gluons (Pomeron). The variable  $\beta$  is used in  $Q\bar{Q}$  production. In this case the effective mass of a produced quark system is equal to  $M_X^2 = (q + r_P)^2$  and can be quite large. The variable  $\beta = x/x_P \sim Q^2/(M_X^2 + Q^2)$  can vary here from 0 to 1. For diffractive vector meson production,  $M_X^2 = M_V^2$  and  $\beta \sim 1$  for large  $Q^2$ . From the mass-shell equation for the vector-meson momentum  $V^2 = (q + r_P)^2 = M_V^2$  we find that for these reactions

$$x_P \sim \frac{m_V^2 + Q^2 + |t|}{sy} \quad (3)$$

and is small at high energies. This variable is not fixed for  $Q\bar{Q}$  production.

We shall use the center of mass system of the photon and proton. The spin-average and spin dependent cross sections with parallel and antiparallel longitudinal polarization of a lepton and a proton are determined by

$$\sigma(\pm) = \frac{1}{2} (\sigma(\vec{\leftarrow}) \pm \sigma(\vec{\rightarrow})). \quad (4)$$

They can be expressed in terms of the vector meson photoproduction helicity amplitude  $M_{\mu'\lambda',\mu\lambda}$ , where  $\mu$  and  $\lambda$  are the photon and initial proton polarization,  $\mu'$  and  $\lambda'$  are the vector meson and final proton polarization.

For the cross section integrated over the azimuthal angle between lepton and hadron scattering plane we have

$$\sigma(+) = N \left[ \sum_{\mu',\lambda',\lambda} |M_{\mu'\lambda',+1\lambda}|^2 + \epsilon \sum_{\mu',\lambda',\lambda} |M_{\mu'\lambda',0\lambda}|^2 \right] \quad (5)$$

and

$$\sigma(-) = -N \sqrt{1-\epsilon^2} \sum_{\mu',\lambda'} \left( |M_{\mu'\lambda',+1\frac{1}{2}}|^2 - |M_{\mu'\lambda',+1-\frac{1}{2}}|^2 \right). \quad (6)$$

Here  $\epsilon \simeq 2(1-y)/(1+(1-y)^2)$  is a virtual photon polarization.

The leading contribution to the spin-average cross section can be estimated as

$$\sigma(+) \sim |M_{+1\frac{1}{2},+1\frac{1}{2}}|^2 + \epsilon |M_{0\frac{1}{2},0\frac{1}{2}}|^2. \quad (7)$$

The photons with longitudinal and transverse polarization contribute here.

On the other hand, we find that only transversely polarized photons contribute to the spin-dependent cross section

$$\sigma(-) \sim \sqrt{1-\epsilon^2} \left( |M_{+1\frac{1}{2},+1\frac{1}{2}}|^2 - |M_{+1-\frac{1}{2},+1-\frac{1}{2}}|^2 \right). \quad (8)$$

The model analysis of the amplitudes with different photon and vector meson polarization shows that [13]

$$\frac{|M_{+1\frac{1}{2},+1\frac{1}{2}}|}{|M_{0\frac{1}{2},0\frac{1}{2}}|} \sim 0.6; \quad \frac{|M_{0\frac{1}{2},+1\frac{1}{2}}|}{|M_{0\frac{1}{2},0\frac{1}{2}}|} \sim 0.12; \quad \frac{|M_{+1\frac{1}{2},0\frac{1}{2}}|}{|M_{0\frac{1}{2},0\frac{1}{2}}|} \sim 0.06. \quad (9)$$

Such amplitude hierarchy does not contradict the experimental data on the polarized density matrix elements [6] of the vector meson production. Thus, we can conclude that the amplitude with transversally polarized photons is very important in spin observables. Unfortunately, for the light meson production, these amplitudes are determined by the higher twist effects and are not well defined because of the present infrared singularities [21].

The photoproduction amplitude of longitudinally polarized vector meson can be written in the factorized form [1]

$$M_{0\lambda',\mu\lambda} \propto \int \frac{dX}{X(X-\zeta-i\epsilon)} \langle \lambda' | F_{\rho 1, \rho 2}(X, \zeta, t, \dots) | \lambda \rangle H_{0,\mu}^{\rho 1, \rho 2}(Q, k1, k2, \dots). \quad (10)$$

Here  $F(X, \zeta, \dots)$  is the soft part which can be determined in terms of skewed parton distributions (SPD) and the hard part  $H(X, \dots)$  can be calculated perturbatively.

We can insert the  $g^{\rho\rho'}$  tensor in the intermediate state which can be decomposed in the axial gauge as

$$g^{\rho\rho'} = \sum_{\nu} \epsilon^{\rho}(k, \nu) \epsilon^{*\rho'}(k, \nu). \quad (11)$$

Here gluons are transversally polarized. The hard scattering amplitudes are now determined by the relation

$$H_{0\nu', \mu\nu} = \epsilon_{\rho 1}^*(k2, \nu') H_{0, \mu}^{\rho 1, \rho 2} \epsilon_{\rho 2}(k1, \nu). \quad (12)$$

We suppose that the gluon helicity flip is suppressed and  $\nu = \nu'$ . In this case we can write [15]

$$\epsilon^{*\rho 2}(k1, \nu) \epsilon^{\rho 1}(k2, \nu) = \frac{1}{2} (g_{\perp}^{\rho 1 \rho 2} + \nu \mathcal{P}^{\rho 1 \rho 2}). \quad (13)$$

The symmetric and asymmetric parts of gluon SPD (14) can be decomposed into the following structures:

$$\begin{aligned} \langle \lambda' | F_{\rho 1, \rho 2} | \lambda \rangle g_{\perp}^{\rho 1 \rho 2} &= \frac{\langle \lambda' | \hat{q}' | \lambda \rangle}{p \cdot q'} \mathcal{F}_{\zeta}^g(X, t) + \frac{i}{2m} \frac{\langle \lambda' | \sigma_{\mu\nu} | \lambda \rangle q'^{\mu} r^{\nu}}{p \cdot q'} \mathcal{K}_{\zeta}^g(X, t) \\ \langle \lambda' | F_{\rho 1, \rho 2} | \lambda \rangle \mathcal{P}^{\rho 1 \rho 2} &= \frac{\langle \lambda' | \hat{q}' \gamma_5 | \lambda \rangle}{p \cdot q'} \mathcal{G}_{\zeta}^g(X, t). \end{aligned} \quad (14)$$

For zero momentum transfer one can find that [1]

$$M_{0\frac{1}{2}, 0\frac{1}{2}} = N \frac{1}{Q} \frac{\langle \lambda' | \hat{q}' | \lambda \rangle}{p \cdot q'} f_V \int_0^1 d\tau \frac{\Phi_V(\tau)}{\tau(1-\tau)} \int \frac{dX \mathcal{F}_{\zeta}^g(X, t)}{X(X - \zeta - i\epsilon)}. \quad (15)$$

The Im part of the amplitude is predominated at high energies and has the form

$$M_{0\frac{1}{2}, 0\frac{1}{2}} \sim \text{Im} M_{0\frac{1}{2}, 0\frac{1}{2}} \propto H_0 \frac{\mathcal{F}_{\zeta}^g(\zeta, t)}{\zeta}. \quad (16)$$

Here  $H_0 = H_{0+, 0+}$  is the amplitude with positive gluon polarization.

The cross sections for nonzero  $|t|$  looks like

$$\sigma(+) \sim H_0^2 \left[ \mathcal{F}_{\zeta}^g(\zeta, t)^2 + \frac{|t|}{m^2} \mathcal{K}_{\zeta}^g(\zeta, t)^2 \right]. \quad (17)$$

The spin-dependent cross section for a longitudinally polarized target is expressed through  $\mathcal{G}_{\zeta}^g(X, t)$ .

### 3 Two-gluon exchange model

Now let us study the process of the hadron leptonproduction within the two-gluon exchange model. As we have discussed previously, this contribution is predominated

at small  $x \leq 0.1$ . For larger  $x$  the quark exchange should be included for processes with light quarks. The cross section of hadron leptonproduction can be decomposed into the leptonic and hadronic tensors and the amplitude of hadron production through the  $\gamma^* gg$  transition to the vector meson or  $Q\bar{Q}$  states. To study spin effects in diffractive hadron production, one must know the structure of the two-gluon coupling with the proton at small  $x$ .

It has been shown in [22] that the leading contribution like  $\alpha_s [\alpha_s \ln(1/x)]^n$  to the Pomeron is determined by the gluon ladder graphs. The two-gluon coupling with the proton can be parametrized in the form [23]

$$\begin{aligned} V_{pgg}^{\alpha\beta}(p, t, x_P, l_\perp) &= B(t, x_P, l_\perp)(\gamma^\alpha p^\beta + \gamma^\beta p^\alpha) \\ &+ \frac{iK(t, x_P, l_\perp)}{2m}(p^\alpha \sigma^{\beta\gamma} r_\gamma + p^\beta \sigma^{\alpha\gamma} r_\gamma) + \dots \end{aligned} \quad (18)$$

Here  $m$  is the proton mass. In the matrix structure (18) we wrote only the terms with the maximal powers of a large proton momentum  $p$  which are symmetric in the gluon indices  $\alpha, \beta$ . The structure proportional to  $B(t, \dots)$  determines the spin-non-flip contribution. The term  $\propto K(t, \dots)$  leads to the transverse spin-flip at the vertex. If one considers the longitudinal spin effects, the asymmetric structure  $\propto \gamma_\rho \gamma_5$  should be included in (18).

In what follows, we analyze the  $\gamma^* gg \rightarrow Q\bar{Q}$  transition amplitude. The typical momentum of quarks is proportional to the photon momentum  $q$ . In the Feynman gauge, we can decompose the  $g_{\mu\nu}$  tensors from  $t$ -channel gluons into the longitudinal and transverse parts [22]

$$g^{\alpha\alpha'} = g_l^{\alpha\alpha'} + g_\perp^{\alpha\alpha'} \text{ with } g_l^{\alpha\alpha'} \sim \frac{q^\alpha p^{\alpha'}}{(pq)}. \quad (19)$$

The product of the  $g_l^{\alpha\alpha'}$  tensors and the two-gluon coupling of the proton can be written in the form

$$g_l^{\alpha'\alpha} g_l^{\beta'\beta} V_{pgg}^{\alpha\beta}(p, t, x_P, l_\perp) \propto p^{\alpha'} p^{\beta'} \left[ \frac{\not{q}}{p \cdot q} B(t, x_P, l_\perp) + \frac{iK(t, x_P, l_\perp)}{2m p \cdot q} \sigma^{\beta\gamma} q_\beta r_\gamma \right]. \quad (20)$$

It can be seen that the structure in the square brackets in (20) after integration over the gluon momentum  $l_\perp$  should be related directly to the skewed gluon distribution (14)

$$\mathcal{F}_\zeta^g(\zeta, t) \propto \int d^2 l_\perp B(t, \zeta = x_P, l_\perp) \phi(l_\perp, \dots). \quad (21)$$

A similar equation should be valid for the  $K$  function. The function  $\phi$  will be found later.

In what follows we will calculate directly the spin dependent cross section of hadron production which can be expressed in terms of the hard hadron production amplitude through photon-gluon fusion convoluted with the spin-dependent hadron and lepton tensors. The structure of the leptonic tensor is simple because the lepton

is a point-like object

$$\begin{aligned}\mathcal{L}^{\mu\nu}(s_l) &= \sum_{spin\ s_f} \bar{u}(l', s_f) \gamma^\mu u(l, s_l) \bar{u}(l, s_l) \gamma^\nu u(l', s_f) \\ &= \text{Tr} \left[ (\not{l} + \mu) \frac{1 + \gamma_5 \not{s}_l}{2} \gamma^\nu (\not{l}' + \mu) \gamma^\mu \right],\end{aligned}\quad (22)$$

where  $l$  and  $l'$  are the initial and final lepton momenta, and  $s_l$  is a spin vector of the initial lepton.

Spin-average and spin-dependent lepton tensors are defined by

$$\mathcal{L}^{\mu\nu}(\pm) = \frac{1}{2} (\mathcal{L}^{\mu\nu}(\pm \frac{1}{2}) \pm \mathcal{L}^{\mu\nu}(-\frac{1}{2})). \quad (23)$$

The  $\mathcal{L}^{\mu\nu}(\pm \frac{1}{2})$  are the tensors with helicity of the initial lepton equal to  $\pm 1/2$  and

$$\begin{aligned}\mathcal{L}^{\mu\nu}(+) &= 2(g^{\mu\nu} l \cdot q + 2l^\mu l^\nu - l^\mu q^\nu - l^\nu q^\mu), \\ \mathcal{L}^{\mu\nu}(-) &= 2i\mu\epsilon^{\mu\nu\delta\rho} q_\delta(s_l)_\rho.\end{aligned}\quad (24)$$

The hadronic tensor is given by a trace similar to the lepton case (22)

$$\begin{aligned}W^{\alpha\alpha';\beta\beta'}(s_p) &= \sum_{spin\ s_f} \bar{u}(p', s_f) V_{pgg}^{\alpha\alpha'}(p, t, x_P, l) u(p, s_p) \\ &\quad \bar{u}(p, s_p) V_{pgg}^{\beta\beta'}(p, t, x_P, l') u(p', s_f).\end{aligned}\quad (25)$$

The spin-average and spin-dependent hadron tensors look like

$$W^{\alpha\alpha';\beta\beta'}(\pm) = \frac{1}{2} (W^{\alpha\alpha';\beta\beta'}(+s_p) \pm W^{\alpha\alpha';\beta\beta'}(-s_p)). \quad (26)$$

Here  $s_p$  is the spin vector which determines the target polarization. For the leading term of the spin- average structure  $W(+)$  for the ansatz (18) we find

$$W^{\alpha\alpha';\beta\beta'}(+) = 16p^\alpha p^{\alpha'} p^\beta p^{\beta'} (|B|^2 + \frac{|t|}{m^2} |K|^2). \quad (27)$$

The spin-dependent part of the hadron tensor is more complicated. Its explicit form can be found in [23]

The obtained equation for the spin-average tensor coincides in form with the cross section of the proton off the spinless particle (a meson, e.g.). Really, the meson-proton helicity-non-flip and helicity-flip amplitudes can be written in terms of the invariant functions  $\tilde{B}$  and  $\tilde{K}$  which describe spin-non-flip and spin-flip effects

$$F_{++}(s, t) = is[\tilde{B}(t)]f(t); \quad F_{+-}(s, t) = is\frac{\sqrt{|t|}}{m}\tilde{K}(t)f(t), \quad (28)$$

where  $f(t)$  is determined by the Pomeron coupling with meson. The functions  $\tilde{B}$  and  $\tilde{K}$  are defined by integrals like (21). The cross-section is written in the form

$$\frac{d\sigma}{dt} \sim [|\tilde{B}(t)|^2 + \frac{|t|}{m^2} |\tilde{K}(t)|^2] f(t)^2. \quad (29)$$

The term proportional to  $\tilde{B}$  represents the standard Pomeron coupling that leads to the non-flip amplitude. The  $\tilde{K}$  function is the spin-dependent part of the Pomeron coupling which produces in our case the transverse spin-flip effects in the proton.

There are some models that provide spin-flip effects which do not vanish at high energies. In the model [24], the amplitudes  $K$  and  $B$  have a phase shift caused by the soft Pomeron rescattering effect. The vector diquark in the diquark model [25] generates the  $K$  amplitude which is out of phase with the Pomeron contribution to the amplitude  $B$ . The models [24, 25] describe the experimental data [26] on single spin transverse asymmetry  $A_N$  quite well. Thus, the weak energy dependence of spin asymmetries in exclusive reactions is not now in contradiction with the experiment [24, 27]. The model [24] predicts large negative value of  $A_N$  asymmetry near the diffraction minimum which has a weak  $s$  dependence in the RHIC energy range and  $A_N$  is of about 10% for  $|t| \sim 3\text{GeV}^2$  (Fig.1). Some other model predictions for single-spin asymmetry at small momentum transfer have been discussed in [28]. Thus, it should be important to measure experimentally (PP2PP at RHIC) the transverse asymmetry in the vicinity of diffraction minimum, which is very sensitive to the imaginary part of the spin-flip  $K$  amplitude. This can give direct information about the energy dependence of the spin-flip amplitude  $K$ .

It has been found in [25, 24] that the ratio  $|\tilde{K}|/|\tilde{B}| \sim 0.1$  and has a weak energy dependence. We shall use this value for our estimations of the asymmetry in diffractive hadron production.

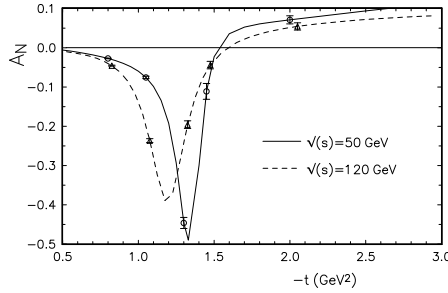


Fig. 1. Predictions of the model [24] for single-spin transverse asymmetry of the  $pp$  scattering at RHIC energies [27]. Error bar indicates expected statistical errors for the PP2PP experiment at RHIC.

#### 4 Diffractive Vector Meson Leptonproduction

Vector meson production through the photon-two gluon fusion is shown in Fig.2. We regard mainly the  $J/\Psi$  meson production where such effects are predominated. The  $J/\Psi$  meson can be considered as a  $S$ -wave system of heavy quarks with the

wave function of the form

$$\Psi_V = g(\not{k} + m_q)\gamma_\mu \quad (30)$$

where  $k$  is the momentum of a quark, and  $m_q$  is its mass. In the nonrelativistic approximation the quarks have the same momenta  $k = V/2$  and the mass  $m_q = m_J/2$ . The transverse quark motion is not considered. This means that the vector meson distribution amplitude has a simple form  $\delta(\tau - 1/2)\delta(k_t^2)$ . The wave function (30) for nonzero mass  $m_q$  produces both amplitudes with a longitudinally and transversely polarized vector meson. For the light meson production  $m_q = 0$ , and one must consider the higher twist effects to calculate the amplitude with transverse vector meson polarization (see e.g. [16]).

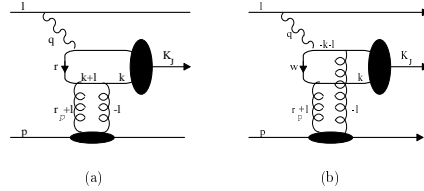


Fig. 2. Two-gluon contribution to diffractive vector meson production.

The spin-average and spin-dependent cross-sections are defined as

$$d\sigma(\pm) = \frac{1}{2} (d\sigma(\rightarrow\downarrow) \pm d\sigma(\rightarrow\uparrow)). \quad (31)$$

The cross section  $d\sigma(\pm)$  can be written in the form

$$\frac{d\sigma^\pm}{dQ^2 dy dt} = \frac{|T^\pm|^2}{32(2\pi)^3 Q^4 s^2 y}. \quad (32)$$

For the spin-average amplitude squared we find

$$|T^+|^2 = \frac{s^2 N}{4Q^4} ((1 + (1 - y)^2)m_V^2 + 2(1 - y)Q^2) \left[ |\tilde{B}|^2 + |\tilde{K}|^2 \frac{|t|}{m^2} \right]. \quad (33)$$

Here  $\bar{Q}^2 = (m_V^2 + Q^2 + |t|)/4$ , and  $N$  is the normalization factor. The term proportional to  $(1 + (1 - y)^2)m_V^2$  represents the contribution of the transversely polarized photons. The  $2(1 - y)Q^2$  term describes the effect of longitudinal photons (see (7)).

The function  $\tilde{B}$  is determined by

$$\begin{aligned} \tilde{B} = \bar{Q}^2 \int \frac{d^2 l_\perp (l_\perp^2 + \vec{l}_\perp \vec{r}_\perp) B(t, l_\perp^2, x_P, \dots)}{(l_\perp^2 + \lambda^2)((\vec{l}_\perp + \vec{\Delta})^2 + \lambda^2)[l_\perp^2 + \vec{l}_\perp \vec{r}_\perp + \bar{Q}^2]} \sim \\ \int_0^{l_\perp^2 < \bar{Q}^2} \frac{d^2 l_\perp (l_\perp^2 + \vec{l}_\perp \vec{r}_\perp)}{(l_\perp^2 + \lambda^2)((\vec{l}_\perp + \vec{r}_\perp)^2 + \lambda^2)} B(t, l_\perp^2, x_P, \dots) = \mathcal{F}_{x_P}^g(x_P, t, \bar{Q}^2). \end{aligned} \quad (34)$$



Due to the gauge invariance, the result in the Feynman gauge should be equal to the corresponding result in the axial gauge (section 2). This permits us to find the connection with SPD in (34) by a direct comparison of the cross section (32) with (17). We can see that the  $B(l_\perp^2, x_P, \dots)$  function represents the nonintegrated spin-average gluon distribution.

The spin-dependent amplitude squared is found to be of the form

$$|T^-|^2 = \frac{\vec{Q}\vec{S}_\perp}{4m} \frac{s|t|N}{4\bar{Q}^4} (Q^2 + m_V^2 + |t|) \frac{\tilde{B}\tilde{K}^* + \tilde{B}^*\tilde{K}}{2}. \quad (35)$$

It is determined by the interference between the  $\tilde{B}$  and  $\tilde{K}$  amplitudes.

### 5 Diffractive $Q\bar{Q}$ Photoproduction

To study  $Q\bar{Q}$  production we shall use the same two-gluon model which should describe the cross sections at small  $x < 0.1$ . This contribution is shown in Fig. 3. The quark-antiquark contribution, in addition to the  $t$ -channel gluons, is important for light quark production at large  $x$ . To calculate the cross sections, we integrate the

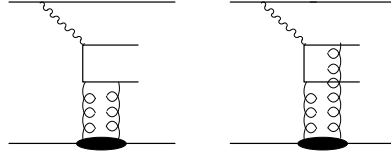


Fig. 3. Two-gluon contribution to  $Q\bar{Q}$  production

amplitudes squared over the  $Q\bar{Q}$  phase space  $dN_{Q\bar{Q}} = \Pi_f \frac{d^3 p_f}{(2\pi)^3 2E_f}$  with the delta function that reflects the momentum conservation. As a result, the spin-average and spin-dependent cross section can be written in the form

$$\frac{d^5\sigma(\pm)}{dQ^2 dy dx_p dt dk_\perp^2} = \binom{(2-2y+y^2)}{(2-y)} \frac{C(x_P, Q^2) N(\pm)}{\sqrt{1 - 4(k_\perp^2 + m_q^2)/M_X^2}}. \quad (36)$$

Here  $C(x_P, Q^2)$  is a normalization function which is common for the spin average and spin dependent cross section;  $N(\pm)$  is determined by a sum of graphs integrated over the gluon momenta  $l$  and  $l'$

$$N(\pm) = \int \frac{d^2 l_\perp d^2 l'_\perp (l_\perp^2 + \vec{l}_\perp \vec{r}_\perp) ((l'_\perp)^2 + \vec{l}'_\perp \vec{r}_\perp) D^\pm(t, Q^2, l_\perp, l'_\perp, \dots)}{(l_\perp^2 + \lambda^2)((\vec{l}_\perp + \vec{r}_\perp)^2 + \lambda^2)(l'^2_\perp + \lambda^2)((\vec{l}'_\perp + \vec{r}_\perp)^2 + \lambda^2)}. \quad (37)$$

The  $D^\pm$  function is a hard part that contains the traces over the quark loops of the graphs convoluted with the spin average and spin-dependent tensors.

The analytic forms of the graph contribution to the cross sections will be written here in the limit  $\beta \rightarrow 0$  for simplicity. The  $D^+$  function has the following form [23]:

$$D_I^+ = \frac{Q^2 (|B|^2 + |t|/m^2 |K|^2) ((k_\perp + r_\perp)^2 + m_q^2)}{(k_\perp^2 + m_q^2) ((k_\perp - l_\perp)^2 + m_q^2) ((k_\perp - l'_\perp)^2 + m_q^2)}. \quad (38)$$

This function contains a product of the off-mass-shell quark propagators in the graphs. We can see that the quark virtuality here is quite different as compared to the vector meson case. We have no terms proportional to  $Q^2$  (see (34)). This will change the scale in gluon structure functions. Really,  $l$  and  $l'$  are smaller than  $k_\perp^2$  and the contribution of  $D^p(+)$  to  $N(+)$  is about

$$N^p(+)\sim \frac{(|\tilde{B}|^2 + |t|/m^2 |\tilde{K}|^2) ((k_\perp + r_\perp)^2 + m_q^2)}{(k_\perp^2 + m_q^2)^3} \quad (39)$$

with

$$\begin{aligned} \tilde{B} &\sim \int_0^{l_\perp^2 < k_0^2} \frac{d^2 l_\perp (l_\perp^2 + \vec{l}_\perp \vec{r}_\perp)}{(l_\perp^2 + \lambda^2)((\vec{l}_\perp + \vec{r}_\perp)^2 + \lambda^2)} B(t, l_\perp^2, x_P, \dots) = \mathcal{F}_{x_P}^g(x_P, t, k_0^2) \\ \tilde{K} &\sim \int_0^{l_\perp^2 < k_0^2} \frac{d^2 l_\perp (l_\perp^2 + \vec{l}_\perp \vec{r}_\perp)}{(l_\perp^2 + \lambda^2)((\vec{l}_\perp + \vec{r}_\perp)^2 + \lambda^2)} K(t, l_\perp^2, x_P, \dots) = \mathcal{K}_{x_P}^g(x_P, t, k_0^2), \end{aligned} \quad (40)$$

where  $k_0^2 \sim k_\perp^2 + m_q^2$ . We find that the structure functions are determined by the same integrals as in (34), but with a different scale. The details of calculations can be found in [23]

The contribution of all graphs to the function  $N(+)$  for an arbitrary  $\beta$  can be written as

$$N(+) = \left( |\tilde{B}|^2 + |t|/m^2 |\tilde{K}|^2 \right) \Pi^{(+)}(t, k_\perp^2, Q^2). \quad (41)$$

The function  $\Pi^{(+)}$  will be calculated numerically.

The same analysis was done for the spin-dependent cross sections. In addition to the term observed in (35) and proportional to the scalar production  $\vec{Q}\vec{S}_\perp$ , the new term  $\propto \vec{k}_\perp \vec{S}_\perp$  appears in the spin-dependent part. As a result, we find the following representation of the function  $N(-)$

$$\begin{aligned} N(-) = \sqrt{\frac{|t|}{m^2}} \left( \tilde{B}\tilde{K}^* + \tilde{B}^*\tilde{K} \right) & \left[ \frac{(\vec{Q}\vec{S}_\perp)}{m} \Pi_Q^{(-)}(t, k_\perp^2, Q^2) \right. \\ & \left. + \frac{(\vec{k}_\perp \vec{S}_\perp)}{m} \Pi_k^{(-)}(t, k_\perp^2, Q^2) \right]. \end{aligned} \quad (42)$$

## 6 Numerical Results for Vector Meson production

The spin-average cross section of the vector meson production at a small momentum transfer is approximately proportional to the  $|\tilde{B}|^2$  function (33) which is

connected with the skewed gluon distribution. The simple parameterization of the SPD as a product of the form factor and the ordinary gluon distribution will be used

$$\tilde{B}(t, x_P, \bar{Q}^2) = F_B(t) (x_P G(x_P, \bar{Q}^2)). \quad (43)$$

The form factor  $F_B(t)$  is chosen as an electromagnetic form factor of the proton. Such a simple choice can be justified by that the Pomeron–proton vertex might be similar to the photon–proton coupling

$$F_B(t) \sim F_p^{em}(t) = \frac{(4m_p^2 + 2.8|t|)}{(4m_p^2 + |t|)(1 + |t|/0.7\text{GeV}^2)^2}. \quad (44)$$

The energy dependence of the cross sections is determined by the Pomeron contribution to the gluon distribution function at small  $x$

$$(x_P G(x_P, \bar{Q}^2)) \sim \frac{\text{const}}{x_P^{\alpha_p(t)-1}} \sim \left( \frac{sy}{m_J^2 + Q^2 + |t|} \right)^{(\alpha_p(t)-1)}. \quad (45)$$

Here  $\alpha_p(t)$  is a Pomeron trajectory which is chosen in the form

$$\alpha_p(t) = 1 + \epsilon + \alpha' t \quad (46)$$

with  $\epsilon = 0.15$  and  $\alpha' = 0$ . These values are in accordance with the fit of the diffractive  $J/\Psi$  production by ZEUS [2].

We suppose that the ratio of spin–dependent and spin–average densities has a weak  $x$  dependence and

$$\frac{|\tilde{K}|}{|\tilde{B}|} \sim 0.1 \quad (47)$$

as in the case of elastic scattering. Our prediction for the cross sections is shown in Fig.4.

The  $A_{LT}$  asymmetry for vector meson production is determined by the ratio of cross sections determined in (35,33)

$$A_{LT} \sim \frac{\vec{Q} \vec{S}_\perp}{4m} \frac{yx_P |t|}{(1 + (1-y)^2)m_V^2 + 2(1-y)Q^2} \frac{\tilde{B} \tilde{K}}{|\tilde{B}|^2 + |\tilde{K}|^2 |t|/m^2}. \quad (48)$$

The expected asymmetry for  $J/\Psi$  production at HERMES energies is shown in Fig.5 for the case when the transverse part of the photon momentum is parallel to the target polarization  $S_\perp$ . At the HERA energies, asymmetry will be extremely small.

For a small momentum transfer, this asymmetry can be approximated as

$$A_{LT} \sim C_g \frac{\mathcal{K}_\zeta^g(\zeta)}{\mathcal{F}_\zeta^g(\zeta)} \quad \text{with } \zeta = x_P \quad (49)$$

Simple estimations show that the coefficient  $C_g(J/\Psi)$  at HERMES energy for  $y = 0.5, |t| = 1\text{GeV}^2, Q^2 = 5\text{GeV}^2$  is quite small, about 0.007.

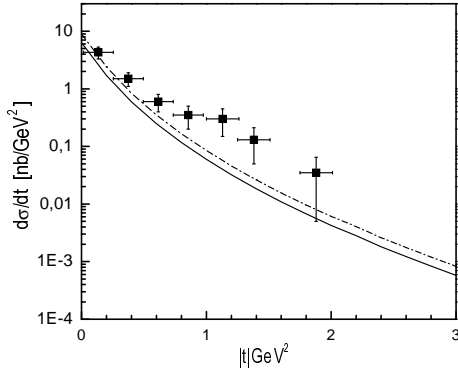


Fig. 4. The differential cross section of  $J/\Psi$  production at HERA energy: solid line -for  $|\tilde{K}|/|\tilde{B}| = 0$ ; dot-dashed line -for  $|\tilde{K}|/|\tilde{B}| = 0.1$ . Data are from [3].

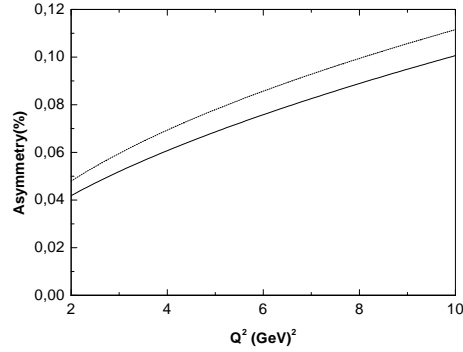


Fig. 5. The  $A_{lT}$  asymmetry for vector meson production at  $\sqrt{s} = 7\text{GeV}$  ( $y=0.5$ ,  $|t| = 1\text{GeV}^2$ ): solid line -for  $J/\Psi$  production; dotted line -for  $\rho$  production.

For light vector mesons, we use the same Eq. (48). The model predicts a weak mass dependence of the gluon contribution to the asymmetry, Fig.5. For the same kinematic variables,  $C(\phi) \sim C(\rho) \sim 0.008$ . Note that this result was obtained for the nonrelativistic meson wave function in the form  $\delta(\tau - 1/2)\delta(k_t^2)$  which is not a good approximation for light meson production. It is important to study a more realistic wave function which takes into consideration the transverse quark degrees of freedom.

## 7 Predictions for $Q\bar{Q}$ Leptoproduction

We shall now discuss our prediction for polarized diffractive  $Q\bar{Q}$  production. In estimations of the asymmetry  $A_{lT} = \sigma(-)/\sigma(+)$  we shall use the same parameterizations of SPD as in (43) with the functions determined in (44). As in the case of vector meson production, the asymmetry is approximately proportional to the ratio of polarized and spin-average gluon distribution functions

$$A_{LT}^{Q\bar{Q}} \sim C^{Q\bar{Q}} \frac{\mathcal{K}_\zeta^g(\zeta)}{\mathcal{F}_\zeta^g(\zeta)} \quad \text{with } \zeta = x_P \text{ and } |\tilde{K}|/|\tilde{B}| \sim 0.1 \quad (50)$$

The spin-dependent contribution to the asymmetry which is proportional to  $\vec{k}_\perp \vec{S}_\perp$  will be analyzed for the case when the transverse jet momentum  $\vec{k}_\perp$  is parallel to the target polarization  $\vec{S}_\perp$ . The asymmetry is maximal in this case. To observe this contribution to asymmetry, it is necessary to distinguish experimentally the quark and antiquark jets. This can be realized presumably by the charge of the leading particles in the jet which should be connected in charge with the quark produced in the photon-gluon fusion. If we do not separate events with  $\vec{k}_\perp$  for the quark jet, e.g., the resulting asymmetry will be equal to zero because the

transverse momentum of the quark and antiquark are equal and opposite in sign.

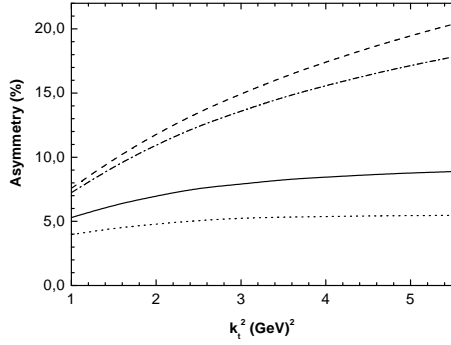


Fig. 6. The  $A_{IT}^k$  asymmetry in diffractive heavy  $Q\bar{Q}$  production at  $\sqrt{s} = 20\text{GeV}$  for  $x_P = 0.1$ ,  $y = 0.5$ ,  $|t| = 0.3\text{GeV}^2$ : dotted line-for  $Q^2 = 0.5\text{GeV}^2$ ; solid line-for  $Q^2 = 1\text{GeV}^2$ ; dot-dashed line-for  $Q^2 = 5\text{GeV}^2$ ; dashed line-for  $Q^2 = 10\text{GeV}^2$ .

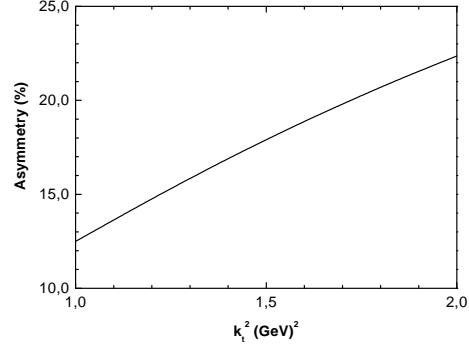


Fig. 7. The  $A_{IT}^k$  asymmetry in diffractive light  $Q\bar{Q}$  production for  $Q^2 = 5\text{GeV}^2$ ,  $x_P = 0.1$ ,  $y = 0.5$ ,  $|t| = 0.3(\text{GeV})^2$  at  $\sqrt{s} = 7\text{GeV}$ .

The spin-dependent cross section vanishes for  $Q^2 \rightarrow 0$ , while the spin-average cross section is constant in this limit. As a result, the  $Q^2$  dependence of the asymmetry can be approximated as  $A_{IT} \propto Q^2/(Q^2 + Q_0^2)$  with  $Q_0^2 \sim 1\text{GeV}^2$ . The predicted asymmetry for heavy  $c\bar{c}$  production at COMPASS energies is shown in Fig.6. The asymmetry for light quark production is approximately of the same order of magnitude. At the low energy  $\sqrt{s} = 7\text{GeV}$  (HERMES) we can work perturbatively only in a very limited region of  $k^2$ . Really,  $k_{\perp}^2$  should be large enough to have a large scale  $k_0^2$  in the process (40). Otherwise, from (36), we have the restriction that  $k^2 \leq M_X^2/4$ . For quite large  $M_X^2 \sim (8 - 10)\text{GeV}^2 \sim M_{J/\psi}^2$  we find that  $(k_{\perp}^2)_{max} \sim 2\text{GeV}^2$ . The expected  $A_{IT}$  asymmetry for light quark production at HERMES is shown in Fig.7. The coefficient  $C_k^{QQ}$  in (50) is quite large, about 1.5 at the HERMES energy for  $k_{\perp}^2 = 1.3\text{GeV}^2$ ,  $Q^2 = 5\text{GeV}^2$ ,  $x_P = 0.1$ ,  $y = 0.5$ , and  $|t| = 0.3\text{GeV}^2$ . This shows a possibility of studying the polarized gluon distribution  $\mathcal{K}_{\zeta}^g(x)$  in the HERMES experiment.

The contribution to asymmetry  $\propto \vec{Q} \vec{S}_{\perp}$  is analyzed for the case when the transverse jet momentum  $\vec{Q}_{\perp}$  is parallel to the target polarization  $\vec{S}_{\perp}$  (a maximal contribution to the asymmetry). The predicted  $A_{IT}^Q$  asymmetry in diffractive heavy  $Q\bar{Q}$  production at  $\sqrt{s} = 20\text{GeV}$  is shown in Fig.8. The  $A_{IT}^Q$  asymmetry has a strong mass dependence. For light quark production, this asymmetry is not small for  $Q^2 \sim (0.5 - 1)\text{GeV}^2$  and positive.

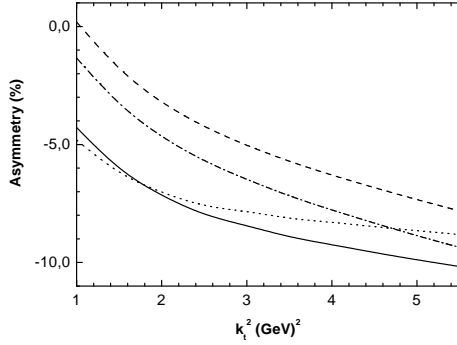


Fig. 8. The  $A_{IT}^Q$  asymmetry in diffractive heavy  $Q\bar{Q}$  production at  $\sqrt{s} = 20\text{GeV}$  for  $x_P = 0.1$ ,  $y = 0.5$ ,  $|t| = 0.3\text{GeV}^2$ : dotted line-for  $Q^2 = 0.5\text{GeV}^2$ ; solid line-for  $Q^2 = 1\text{GeV}^2$ ; dot-dashed line-for  $Q^2 = 5\text{GeV}^2$ ; dashed line-for  $Q^2 = 10\text{GeV}^2$ .

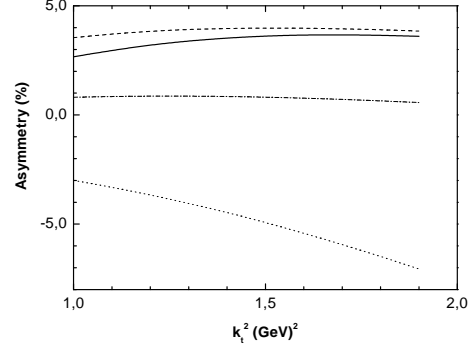


Fig. 9. The  $A_{IT}^Q$  asymmetry in diffractive light  $Q\bar{Q}$  production at  $\sqrt{s} = 7\text{GeV}$  for  $Q^2 = 5\text{GeV}^2$ ,  $x_P = 0.1$ ,  $y = 0.5$ : dotted line -at  $|t| = 0.1\text{GeV}^2$ ; dot-dashed line -at  $|t| = 0.3\text{GeV}^2$ ; dashed line -at  $|t| = 0.5\text{GeV}^2$ ; solid line- integrated over  $|t|$  asymmetry.

It is interesting to look for what we expect to observe for light quark production at low energy  $\sqrt{s} = 7\text{GeV}$ . The predicted asymmetry for different momentum transfers is shown in Fig. 9. Note that in fixed-target experiments, it is usually difficult to detect the final hadron and determine the momentum transfer. In this case, it will be useful to have predictions for the asymmetry integrated over momentum transfer

$$\bar{A}_{IT}^Q = \frac{\int_{t_{min}}^{t_{max}} \sigma(-) dt}{\int_{t_{min}}^{t_{max}} \sigma(+) dt}. \quad (51)$$

We integrate cross sections from  $t_{min} \sim (x_P m)^2 \sim 0$  up to  $t_{max} = 4\text{GeV}^2$ . The predicted integrated asymmetry (see Fig. 9) is not small, about 3%.

## 8 Conclusion

In the present lecture, we analyze diffractive hadron leptonproduction at small  $x$ . Diffractive reactions are predominated in this region by the gluon exchange. We consider two approaches which are used in theoretical estimations of diffractive processes. The first one is based on the factorization of the scattering amplitude into the hard subprocess and soft skewed gluon distribution. The other approach uses the two-gluon exchange model where the cross sections of diffractive hadron production are determined in terms of the leptonic and hadronic tensors and the squared amplitude of hadron production through the photon-two-gluon fusion. The hadronic tensor is expressed in terms of the two-gluon couplings with the proton. The processes of diffractive meson and  $Q\bar{Q}$  production are dependent on the same

integrals over gluon transverse momentum which are related to the gluon SPD  $\mathcal{F}_\zeta(x)$  and  $\mathcal{K}_\zeta(x)$  (34,40).

The diffractive hadron leptonproduction for a longitudinally polarized lepton and a transversely polarized proton at high energies has been studied within the two-gluon exchange model. The  $A_{lT}$  asymmetry is found to be proportional to the ratio of structure functions  $A_{lT} = CK/\mathcal{F}$ . This asymmetry can be used to get information on the transverse distribution  $\mathcal{K}_{x_P}^g(x_P, t)$  from experiment if the coefficient  $C$  is not small. The corresponding coefficient for vector meson production is expected to be quite small  $C_g(J/\Psi) \sim 0.007$  in the HERMES energy range. It is difficult to expect experimental study of such small asymmetry. However, this result was obtained for a simple nonrelativistic form of the vector meson wave function and can be used only for heavy meson production. The light meson production is more complicated and asymmetry in this case can be different. The transverse quark motion and higher twist effects for transversely polarized  $\rho$  meson should be important here.

In the case of  $Q\bar{Q}$  production we have additional transverse variable  $\vec{k}_\perp$ . This produces, in addition to the term  $\vec{Q}\vec{S}_\perp$  in the  $A_{lT}$  asymmetry, the contribution proportional to the scalar product  $\vec{k}_\perp\vec{S}_\perp$  (42). These terms in the asymmetry have different kinematic properties and can be studied independently. The term  $\propto \vec{k}_\perp\vec{S}_\perp$  has a large coefficient  $C_k^{Q\bar{Q}}$  that is predicted to be about 1. Such asymmetry might be an excellent object to study transverse effects in the proton–gluon coupling. However, the experimental study of this asymmetry is not so simple. To find nonzero asymmetry in this case, it is necessary to distinguish quark and antiquark jets and to have a possibility of studying the azimuthal asymmetry structure. The expected  $A_{lT}$  asymmetry for the term  $\propto \vec{Q}\vec{S}_\perp$  is not small too. The predicted coefficient  $C_Q^{Q\bar{Q}}$  in this case is about 0.3. The diffractive  $Q\bar{Q}$  can be investigated in a polarized proton–proton interaction too where the asymmetry of the same order of magnitude as in the lepton–proton case was predicted [29].

The results presented here should be applicable to the reactions with heavy quarks. For processes with light quarks, our predictions can be used in the small  $x$  region ( $x \leq 0.1$  e.g.) where the contribution of quark SPD is expected to be small. In the region of not small  $x \geq 0.1$  the polarized  $u$  and  $d$  quark SPD might be studied together with the gluon distribution in the case of  $\rho$  production. For the  $\phi$  meson production, the strange quark SPD might be analyzed. Such experiments can be conducted at the future HERMES and COMPASS spectrometers for a transversely polarized target. We conclude that important information on the spin–dependent SPD  $\mathcal{K}_\zeta(x)$  at small  $x$  can be obtained from the asymmetries in diffractive hadron leptonproduction for longitudinally polarized lepton and transversely polarized hadron targets.

These lectures were supported in part by the Russian Foundation of Basic Research, Grant 00-02-16696 and by the Blokhintsev–Votruba program.

## References

- [1] A.V. Radyushkin: Phys.Rev. **D56** (1997) 5524; X. Ji: Phys.Rev. **D55** 7114 (1997).
- [2] ZEUS Collab., J. Breitweg et al: Z. Phys, **C75** (1997) 215.
- [3] H1 Collaboration, S. Aid et al: Nucl. Phys. **B472** (1996) 3.
- [4] H1 Collab., C. Adloff et al: Eur. Phys. J. **C10** (1999) 373.
- [5] ZEUS Collab., J. Breitweg et al: Eur. Phys. J. **C5** (1998) 41;  
H1 Collab., C. Adloff et al: Eur. Phys. J. **C6** (1999) 421.
- [6] H1 Collab., C. Adloff et al: Eur. Phys. J. **C103** (2000) 371;  
ZEUS Collab., J. Breitweg et al: Eur. Phys. J. **C12** (2000) 393.
- [7] HERMES Collab., A. Airapetian et al: Phys. Lett. **B513** (2001) 301.
- [8] M.G. Ryskin: Z. Phys. **C57** (1993) 89.
- [9] S.J. Brodsky et al: Phys. Rev. **D50** (1994) 3134;  
L. Frankfurt, W. Koepf, M. Strikman: Phys. Rev. **D57** (1998) 512.
- [10] B. Clerbaux: *Elastic production of Vector Mesons at HERA: study of the scale of the interaction and measurement of the helicity amplitudes*. E-print: hep-ph/9908519.
- [11] M.G. Ryskin, R.G. Roberts, A.D. Martin, E.M. Levin: Z. Phys. **C76** (1997) 231.
- [12] J.L. Cudell, I. Royen: Nucl. Phys. **B545** (1999) 505.
- [13] D.Y. Ivanov, R. Kirshner: Phys. Rev. **D58** (1998) 114026.
- [14] L. Mankiewicz, G. Piller, T. Weigl: Eur. Phys. J. **C5** (1998) 119.
- [15] H.W. Huang, P. Kroll: Eur. Phys. J. **C17** (2000) 423.
- [16] M. Vanttinen, L. Mankiewicz: Phys.Lett. **B434** (1998) 141.
- [17] M.Diehl: Z. Phys. **C66** (1995) 181.
- [18] J. Bartels, C. Ewerz, H. Lotter, M.Wüsthoff: Phys. Lett. **B386** (1996) 389.
- [19] E.M. Levin, A.D. Martin, M.G. Ryskin, T. Teubner: Z. Phys. **C74** (1997) 671.
- [20] B. Lehmann-Dronke, M. Maul, S. Schaefer, E.Stein, A. Schäfer: Phys.Lett. **B457** (1999) 207.
- [21] L. Mankiewicz, G. Piller: Phys. Rev. **D61** (2000) 074013.
- [22] L.V. Gribov, E.M. Levin, M.G. Ryskin: Phys. Rept. **100** (1983) 151.
- [23] S.V. Goloskokov: Euro. Phys. J. **C24** (2002) 413.
- [24] S.V. Goloskokov, S.P. Kuleshov, O.V. Selyugin: Z. Phys. **C50** (1991) 455.
- [25] S.V. Goloskokov, P. Kroll: Phys. Rev. **D60** (1999) 014019.
- [26] G. Fidecaro et al: Phys. Lett. **B76** (1978) 369; **B105** (1981) 309.
- [27] N. Akchurin, S.V. Goloskokov, O.V. Selyugin: Int.J.Mod.Phys. **A14** (1999) 253.
- [28] E. Predazzi: lectures at this conference; A.F. Martini, E. Predazzi: *Diffraction effects in spin-flip pp amplitudes and predictions for relativistic energies*. E-print: hep-ph/0209027.
- [29] S.V.Goloskokov: Phys.Rev. **D53** (1996) 5995.